Relaxation of quasi-two-dimensional electrons in a quantizing magnetic field probed by time-resolved cyclotron resonance

G. A. Khodaparast, D. C. Larrabee, and J. Kono*
Department of Electrical and Computer Engineering, Rice Quantum Institute, and Center for Nanoscale Science and Technology, Rice University, Houston, Texas 77005

D. S. King
Department of Applied Physics, Stanford University, Stanford, California 94305

S. J. Chung† and M. B. Santos
Department of Physics and Astronomy and Center for Semiconductor Physics in Nanostructures, University of Oklahoma, Norman, Oklahoma 73019

(Received 3 May 2002; revised manuscript received 16 September 2002; published 14 January 2003)

We have measured the picosecond time-resolved cyclotron resonance of photogenerated transient carriers in undoped $InSb/Al_{0.09}In_{0.91}Sb$ quantum wells by two-color pump-probe spectroscopy in a magnetic field. The strong conduction-band nonparabolicity of InSb causes the average cyclotron mass of the electrons, which we monitor directly in time, to decrease as the electrons relax towards the band edge. In addition, the nonparabolicity results in multiple resonances due to the strongly energy-dependent mass and *g* factor, allowing us to determine the time evolution of the Fermi-Dirac distribution function for the excited carriers in quantizing magnetic fields.

DOI: 10.1103/PhysRevB.67.035307 PACS number(s): 78.20.Jq, 42.50.Md, 78.30.Fs

I. INTRODUCTION

Two-dimensional (2D) electron systems in high magnetic fields have been studied intensively for the past two decades, exhibiting a fascinating array of electron correlation effects.[1] Equally importantly, they can provide a unique spectroscopic environment that is not achievable in atomic or molecular systems. Landau and Zeeman quantization lead to externally tunable, nearly equally spaced multiple energy levels, or an energy ladder. Various orbital, spin, and combined resonances have been spectroscopically investigated in Landau-quantized systems,[2] especially in two dimensions, providing significant insight into the low-energy quantum dynamics of charge and spin carriers in the frequency domain.

However, there has been very limited success in directly probing carrier dynamics in these ladder systems in the time domain[3–5] with ultrashort and/or intense far-infrared (FIR) pulses. In particular, to our knowledge, there have been no studies on spin relaxation in a 2D system in high magnetic fields, although the corresponding 3D situation is known.[6] Understanding different spin-relaxation mechanisms in confined structures in the presence of spin-orbit coupling is crucial for developing novel spin-based devices.[7]

Here we report results of a picosecond time-resolved cyclotron resonance (TRCR) study of photogenerated electrons in undoped InSb quantum wells (QW's). TRCR is a recently developed spectroscopic method for studying intraband carrier relaxation in a magnetic field.[4] Specifically, this technique allows us to monitor the effective mass of relaxing carriers as a function of time. An ultrashort near-infrared (NIR) pulse creates transient carriers and the subsequent dynamics are probed by a delayed FIR pulse. InSb is an ideal material for TRCR studies. Its small effective mass and large *g* factor result in large Landau and Zeeman splittings; its strongly energy-dependent mass and *g* factor provide a natural mechanism for CR to expose the electron energy distribution, which evolves in time; and its strong spin-orbit coupling makes it an ideal system in which to compare different spin-relaxation mechanisms. Our data unambiguously demonstrated that the (average) electron cyclotron mass decreases as the electrons relax towards the band edge.

Our technique is unique because it is two color (NIR pump/FIR probe), while previous time-resolved[5] and nonlinear[8,9] FIR work on Landau levels in 2D systems was single color. Because CR occurs only across the Fermi energy, the previous studies were applicable only to samples having a large density of 2D carriers present through, e.g., modulation doping. For highly nonparabolic systems, in which different transitions can be resolved at different magnetic fields, only about two spin-split transitions can be excited and probed by one color, prohibiting a thorough study of the carrier distribution. In contrast, the two-color nature of our experiment allows us to create *transient hot carriers* with a wide range of energy and then probe their distribution over all magnetically accessible energy levels. Furthermore, since our technique can be applied to samples in which there are no carriers present at low temperature, it is uniquely positioned to expose the existence or absence of a spin-relaxation bottleneck. Let us specify each state by three quantum numbers, i.e. (n,N,s), where $n=1$, 2 (subband index), $N=0,1,2,\ldots$ (Landau index), and $s=\pm 1/2$ (spin index). A spin bottleneck is predicted for relaxation from the $(1,0,-1/2)$ to the $(1,0,+1/2)$ level. Because the $(1,0,-1/2)$ to $(1,1,-1/2)$ and $(1,0,+1/2)$ to $(1,1,+1/2)$ transitions occur at different magnetic fields due to nonparabolicity, it should be possible at long time delays to distinguish between equally populated $(1,0,-1/2)$ and $(1,0,+1/2)$ levels, which would indicate the presence of the spin bottleneck, and a $(1,0,+1/2)$-dominated resonance, which would demonstrate the absence of the bottleneck.

II. EXPERIMENTAL METHODS

The sample studied was an undoped multiple QW structure, containing 25 periods of 35-nm InSb wells separated by 50-nm-thick $Al_{0.09}In_{0.91}Sb$ barriers, grown by molecular-beam epitaxy on a semi-insulating (001) GaAs substrate. The sample growth procedures and basic sample characteristics have been described previously.[10] Because of the lattice mismatch between the well and the barrier materials ($\sim$0.5%), the wells were under compressive strain. In order to eliminate any effects of photoexcited carriers in the GaAs substrate, we etched away the substrate using bromine and methanol with the sample mounted on a sapphire plate using low-temperature epoxy. We coated the sample surface with semitransparent NiCr ($\sim$20 nm) in order to reduce unwanted Fabry-Perot interference effects.[11]

The experimental setup for the two-color TRCR spectroscopy of this work was similar to that used in our previous work.[4,12,13] The FIR source was the Stanford Picosecond Free-Electron Laser (FEL), which was tunable from 3 to 80 μm and emitted a transform-limited and diffraction-limited pulsed beam with durations between 600 fs and 2 ps and energies as high as 1 μJ. The NIR source was a mode-locked Ti:sapphire laser seeding a Ti:sapphire based regenerative amplifier operating at 800 nm. The FIR and NIR beams were combined by a Pellicle plate and then focused onto the sample, which was placed in an 8-T superconducting magnet with sapphire cold windows and polypropylene room-temperature windows. The measurements were performed in the Faraday geometry at three FIR wavelengths (46, 42, and 38.5 μm) either by varying the time delay at a fixed magnetic field or by varying the magnetic field at a fixed time delay. The FEL produced millisecond macropulses at 10 Hz, which contained picosecond micropulses at 11.8 MHz. The Ti:sapphire oscillator was locked at the seventh harmonic of the FEL micropulse repetition rate, i.e., 82.6 MHz, and our synchronization electronics allowed us to obtain one NIR pulse from the regenerative amplifier for every FIR macropulse. A liquid-helium-cooled Ge:Ga photoconductive detector was used to collect the FIR beam transmitted through the sample.

III. EXPERIMENTAL RESULTS

Figure 1 shows typical TRCR data. The photoinduced transmission change of the FIR probe pulse is plotted as a simultaneous function of magnetic field and time delay in the ranges of 0–8 T and 0–600 ps. The photoinduced transmission change is defined as $(T_0-T)/T_0$, where T_0 is the transmission value before the arrival of the NIR pump pulse. The wavelength of the FIR radiation was 42 μm and the sample temperature was 1.5 K. These data clearly demonstrate the power and usefulness of this unique spectroscopic technique, containing a wealth of information on carrier dynamics in a magnetic field. While time scans at different magnetic fields can provide insight into how intraband carrier relaxation is affected by the applied magnetic field, magnetic-field scans at different time delays exhibit *picosecond time-resolved snapshots of CR spectra* for the photogenerated transient carriers.

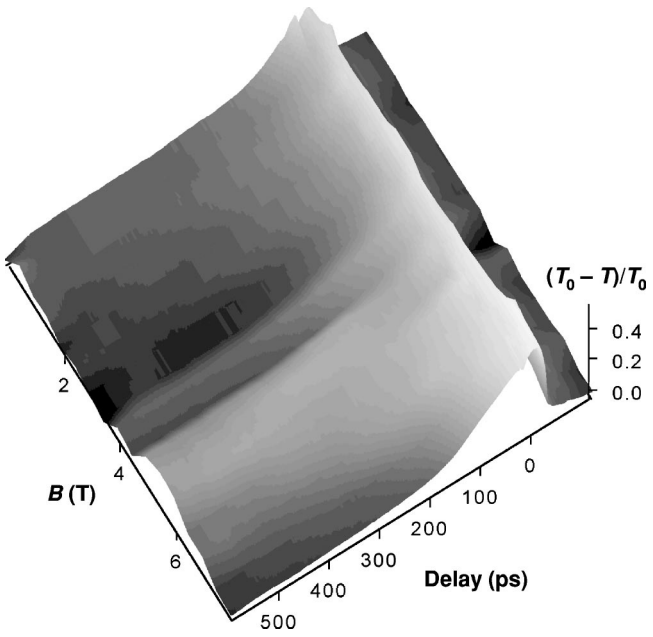

FIG. 1. Picosecond TRCR spectra of photocreated electrons in InSb QW's. The photoinduced transmission change is plotted as a *simultaneous* function of time delay and magnetic field (B). The photoinduced transmission change is defined as $(T_0$-$T)/T_0$, where T_0 is the transmission value before the arrival of the NIR pump pulse. The wavelength of the FIR radiation was 42 μm and the sample temperature was 1.5 K.

Typical magnetic-field scans are shown in Fig. 2(a) for six different fixed time delays. These traces show the smooth evolution of CR from 25 ps to 1.3 ns, a time scale much shorter than the interband lifetime. At 25 ps after excitation, the CR line is significantly broadened to higher B, i.e., to heavier effective mass. As time progresses, the electrons relax towards the band edge, resulting in a lighter mass at 1.3 ns. The average cyclotron mass, total carrier density, and average scattering time, obtained through Lorentzian fits to the traces in Fig. 2(a), are plotted vs delay in Figs. 2(b–d). The resonances observed are fitted best as the sum of two to four Lorentzians, which is consistent with our Landau-level calculations below. We note that the magnetic-field width corresponding to the spectral width of the FEL pulse ($\Delta B \approx 0.087$ T, using $m^*=0.025m_0$, where $m_0=9.11\times10^{-31}$ kg) is much smaller than the width of any of the resonances we observe. The wavelength dependence of the resonance position is consistent with CR.

IV. DISCUSSION

To better understand the TRCR spectra, we calculated energy levels in the QW structure. We first used a four-band $\mathbf{k}\cdot\mathbf{p}$ model in the absence of a magnetic field to calculate the subband energies in the conduction and valence bands by taking into account the energy dependence of the electron and hole masses in the envelope function formalism.[14] We also included strain effects using a method similar to the work by Kurtz and Biefeld on $InAs_xSb_{1-x}$/InSb superlattices.[15] For the 35-nm InSb/50-nm $Al_{0.09}In_{0.91}Sb$ QW

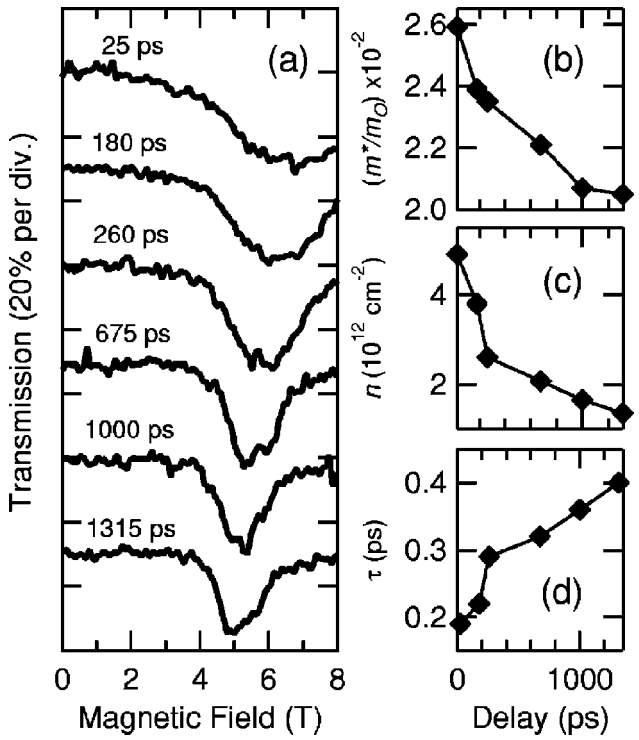

FIG. 2. (a) Transmission change of the FIR probe pulse as a function of magnetic field at different time delays. The wavelength of the probe was 42 μm, the sample temperature was 1.5 K, and the NIR fluence was $\sim$1.3 mJ/cm^2. (b) Average cyclotron mass vs time delay. (c) Total carrier density (n) vs time delay. (d) Average carrier scattering time (τ) vs time delay.

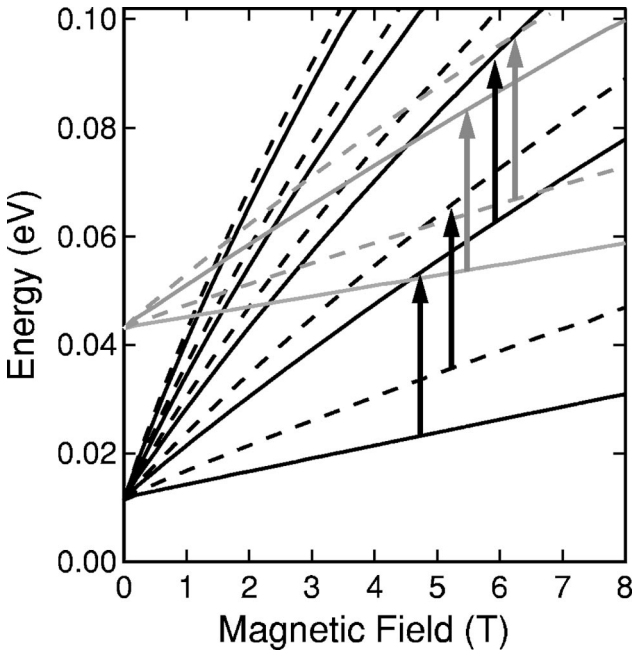

FIG. 3. Conduction-band Landau levels calculated using a modified Pidgeon-Brown model, which takes into account confinement and strain effects. Black (gray) lines are for the first (second) subband. Solid (dashed) lines are spin-up (spin-down) states. The arrows show the possible CR transitions for 42-μm radiation.

structure, we found three subbands in the conduction band with energies 12, 42, and 83 meV, assuming the well and barrier band gaps to be 249 meV and 416 meV, respectively, and the conduction-band offset to be 62% of the band-gap difference.[16] The first three heavy-hole (HH) subband energies were calculated to be 1, 4, and 9.5 meV. The strain in this system gives rise to a large splitting between the HH and light-hole (LH) bands of $\sim$30 meV. For the structure studied here, two LH subbands are expected at 7 and 25 meV below the top of the LH confinement potential.

We took into account a magnetic field applied along the growth direction [001] using a modified Pidgeon-Brown model.[17,18] In this model, the bulk energy gap is replaced by the effective band gap, i.e., the energy separation between the lowest conduction and highest valence subbands. Several calculated low-lying conduction-band Landau levels are shown in Fig. 3, where the black (gray) lines originate from the first (second) subband and solid (dashed) lines represent spin-up (spin-down) states. This calculation shows the strong energy dependence of the g factor and of the effective mass, which cause different transitions to occur at different magnetic fields. We have neglected transitions in the hole bands. However, because the band-edge LH effective mass $(0.016m_0)$ is close to the electron effective mass $(0.0139m_0)$, it is possible that LH CR overlaps electron CR.

The calculated electron energy levels in Fig. 3 strongly suggest that the resonances we observe consist of multiple transitions. The allowed transitions are such that $\Delta n=0$, $\Delta N=1$, and $\Delta s=0$. The electric-field vector of our FIR probe lay in the QW plane and thus did not couple with the intersubband transition $(\Delta n=1)$. Electric-dipole-excited electron spin resonance $(\Delta n,\Delta N,\Delta s)=(0,0,1)$ cannot be observed at the same FIR wavelengths as CR in the magnetic-field range available to us.[19,20] Finally, combined resonance $(\Delta n,\Delta N,\Delta s)=(0,1,1)$ is not allowed in the Faraday geometry.[21] In Fig. 3, the allowed CR transitions for 42-μm probe light in the first and second subbands are indicated by arrows. Because the individual CR transitions are too broad to resolve separately, however, we do not directly observe spin- or Landau-level-resolved CR.

Because different transitions occur at different magnetic fields, it is possible to combine the data and the calculation in Fig. 3 to extract the time evolution of the energy of the excited carrier population. Our detailed simulation of the TRCR spectra obtained for 42-μm probe light is shown in Fig. 4. The fixed parameters in the simulation were the calculated magnetic-field positions of the CR transitions and, at each time delay, the carrier density, which accounts for recombination, and scattering time, taken from fits as in Fig. 2. The scattering time was kept the same for all single-particle resonances at a particular delay. By doing so we are assuming that the same broadening mechanisms act on each transition at the same density. The variable parameter was the temperature of the Fermi-Dirac distribution of the excited carriers. We neglected continuum states above the barrier energy and many-body effects such as band-gap renormalization. We took into account the reduction in CR-active population that occurs when the upper level of a transition is populated. The results accurately reproduced the observed

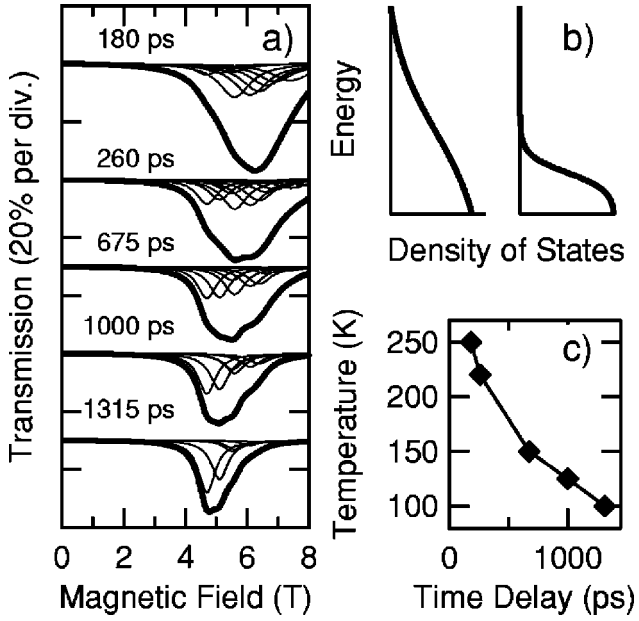

FIG. 4. (a) Simulated TRCR spectra for the traces in Fig. 2, based on the energy levels shown in Fig. 3. Simulation successfully reproduces the main observed features arising from nonparabolicity. (b) Cartoon at left (right) shows a Fermi distribution at short (long) time delay, when the carrier population is large and hot (small and cold). (c) Simulated carrier temperature as a function of time delay.

features, which arise from the strong conduction-band nonparabolicity. Namely, the initially excited carriers, having a high carrier temperature, populate some states with high Landau indices, where the cyclotron masses are higher than that of the lowest electron Landau level. This is the main cause for the significant initial broadening (inhomogeneous broadening). As time progresses, the electrons relax towards the lowest Landau level, and, as a result, the number of transitions contributing to the observed linewidth decreases with time. In addition, the linewidth of individual CR transitions decreases with time. This indicates that each energy level is initially broadened due to the high scattering rate in the high-density and high-temperature regime (homogeneous broadening). As time progresses, both the electron temperature and density decrease, making individual transitions narrower. The simulation was not representative at very short time delays (<200 ps) because it did not include the dynamics of highly excited carriers relaxing into the well. The simulation, Landau-level calculation, and fittings are consistent with each other, indicating that our single-particle analysis is valid and that Coulomb collapse of the nonparabolicity-induced CR splitting is not present.

The simultaneous determination of the scattering lifetime (τ) and carrier temperature (T_c) as functions of time delay allows us to study the relation between scattering and cooling. Cooling occurs through energy transfer from the carrier system to the lattice, most importantly through longitudinal optical (LO) phonon emission in polar semiconductors such as InSb. Based on the simulated carrier temperatures, we have calculated the scattering times *expected from LO phonon emission alone*, assuming $1/\tau=(1/\tau_{\mathrm{LO}})\exp(-\hbar\omega_{\mathrm{LO}}/k_B T_c)$. Here $1/\tau_{\mathrm{LO}}$ is a material parameter given by $(e^2/8\hbar^2)\sqrt{2m^*\hbar\omega_{\mathrm{LO}}}(\epsilon_\infty^{-1}-\epsilon_0^{-1})$ in 2D,[22] where m^* is the carrier mass, and ϵ_∞ and ϵ_0 are the optical and static dielectric permittivities, respectively. For InSb, τ_{LO} can be estimated to be ~ 400 fs in 2D. In this simple model, we obtained $\tau\sim 5$ ps at 25 ps delay time, which increased smoothly to 61 ps at 1300-ps delay. Hence, the scattering time due to LO phonons is almost two orders of magnitude larger than the scattering times deduced from the fitting [see Fig. 2(d)], indicating that some other scattering mechanism is dominant. While there are a number of possible scattering mechanisms, the most important one, especially in the early high-density regime, is carrier-carrier scattering.[23] Our recent TRCR work on *bulk* InSb (Ref. 13) clearly showed that this is the main scattering mechanism, and it is consistent with the observation that the scattering time is roughly inversely proportional to the density.[13,23] A full treatment of carrier scattering and cooling mechanisms will be given separately.[24]

V. CONCLUSIONS AND FUTURE WORK

In summary, we have performed picosecond two-color (NIR and FIR) time-resolved cyclotron resonance spectroscopy on undoped InSb/AlInSb quantum wells. We monitored the dynamics of FIR transmission while we varied the magnetic field and the time delay between the NIR and FIR pulses. The strong nonparabolicity of the InSb conduction band allowed us to study the relaxation dynamics of quasi-2D electrons in a quantizing magnetic field in unprecedented detail. Specifically, we successfully determined the time evolution of the Fermi-Dirac distribution function of a photogenerated 2D plasma in a magnetic field.

These observations promise interesting future studies using the TRCR technique. For instance, we expect a faster relaxation time when the probe is resonant with the optical phonon energy ($\omega_{\mathrm{LO}}\sim 0.024$ eV$=52$ μm), the phonon energy divided by an integer,[5,8,9] or an integer times the phonon energy. It is possible for us to investigate this intriguing regime using the equipment available to us ($\lambda_{\mathrm{FIR}}=26$ μm). Finally, we point out that the present results suggest the possible use of TRCR for studying spin relaxation near the quantum limit at low densities and in high magnetic fields, where relaxation slowdown and even quenching are predicted. Further efforts are in progress to observe such unusual phenomena.

ACKNOWLEDGMENTS

J.K. gratefully acknowledges support from NSF DMR-0049024, DMR-0134058 (CAREER), DARPA MDA972-00-1-0034 (SPINS), AFOSR F49620-00-1-0349 (MFEL), the Japan Science and Technology Corporation PRESTO Program, and NEDO. M.B.S. thanks NSF for support through DMR-9973167 and DMR-0080054. D.S.K. thanks J. S. Harris for support. We are grateful to S. Q. Murphy for the low-temperature epoxy and to H. A. Schwettman, T. I. Smith, R. L. Swent, T. Kimura, G. A. Marcus, B. Armstrong, and D. Keegan for their technical support during this work at the Stanford Picosecond Free Electron Laser Center.

*Author to whom correspondence should be addressed. URL:http://www.ece.rice.edu/~kono; Electronic address: kono@rice.edu

†Present address: Agilent Technologies, Palo Alto, California.

[1] For a recent review, see, e.g., *Perspectives in Quantum Hall Effects*, edited by S. Das Sarma and A. Pinczuk (Wiley, New York, 1997).

[2] See, e.g., in *Landau Level Spectroscopy*, edited by G. Landwehr and E. I. Rashba, Modern Problems in Condensed Matter Sciences, Vols. 27.1 and 27.2 (North-Holland, Amsterdam, 1991).

[3] D. Some and A.V. Nurmikko, Phys. Rev. B **50**, 5783 (1994).

[4] J. Kono, A.H. Chin, A.P. Mitchell, T. Takahashi, and H. Akiyama, Appl. Phys. Lett. **75**, 1119 (1999).

[5] B.N. Murdin, A.R. Hollingworth, M. Kamal-Saadi, R.T. Kotitschke, C.M. Ciesla, C.R. Pidgeon, P.C. Findlay, H.P.M. Pellemans, C.J.G.M. Langerak, A.C. Rowe, R.A. Stradling, and E. Gornik, Phys. Rev. B **59**, R7817 (1999).

[6] P. Boguslawski and W. Zawadzki, J. Phys. C **13**, 3933 (1980).

[7] S.A. Wolf, D.D. Awschalom, R.A. Buhrman, J.M. Daughton, S. von Molnar, M.L. Roukes, A.Y. Chtchelkanova, and D.M. Treger, Science **294**, 5546 (2001).

[8] T.A. Vaughan, R.J. Nicholas, C.J.G.M. Langerak, B.N. Murdin, C.R. Pidgeon, N.J. Mason, and P.J. Walker, Phys. Rev. B **53**, 16 481 (1996).

[9] S.K. Singh, B.D. McCombe, J. Kono, S.J. Allen, I. Lo, W.C. Mitchel, and C.E. Stutz, Phys. Rev. B **58**, 7286 (1998).

[10] N. Dai, F. Brown, P. Barsic, G.A. Khodaparast, R.E. Doezema, M.B. Johnson, S.J. Chung, K.J. Goldammer, and M.B. Santos, Appl. Phys. Lett. **73**, 1101 (1998).

[11] S.W. McKnight, K.P. Stewart, H.D. Drew, and K. Morrjant, Infrared Phys. **27**, 327 (1987).

[12] M.A. Zudov, J. Kono, A.P. Mitchell, and A.H. Chin, Phys. Rev. B **64**, 121204(R) (2001).

[13] M.A. Zudov, A.P. Mitchell, A.H. Chin, and J. Kono, cond-mat/0209047 (unpublished).

[14] See, e.g., G. Bastard, *Wave Mechanics Applied to Semiconductor Heterostructures* (Les Editions de Physique, Les Ulis, 1988).

[15] S.R. Kurtz and R.M. Biefeld, Phys. Rev. B **44**, 1143 (1991).

[16] N. Dai, G.A. Khodaparast, F. Brown, R.E. Doezema, S.J. Chung, and M.B. Santos, Appl. Phys. Lett. **76**, 3905 (2000).

[17] C.R. Pidgeon and R.N. Brown, Phys. Rev. **146**, 575 (1966).

[18] M.J. Yang, R.J. Wagner, B.V. Shanabrook, J.R. Waterman, and W.J. Moore, Phys. Rev. B **47**, 6807 (1993).

[19] G. A. Khodaparast, R. E. Doezema, S. J. Chung, K. J. Goldammer, and M. B. Santos, in *Proceedings of 10th International Conference on Narrow Gap Semiconductors*, edited by N. Miura, S. Yamada, and S. Takeyama, IPAP Conference Series 2 (Institute of Pure and Applied Physics, Tokyo, 2000), pp. 245–247.

[20] B.D. McCombe and R.J. Wagner, Phys. Rev. B **4**, 1285 (1971).

[21] B.D. McCombe, S.G. Bishop, and R. Kaplan, Phys. Rev. Lett. **18**, 748 (1967).

[22] S. Das Sarma, in *Hot Carriers in Semiconductor Nanostructures: Physics and Applications*, edited by J. Shah (Academic Press, Boston, 1992), pp. 53–85.

[23] B. K. Ridley, *Quantum Processes in Semiconductors*, 4th ed. (Oxford University Press, New York, 1999), Chap. 6.

[24] D. C. Larrabee *et al.* (unpublished).